Tomographic 2-D Gamma Scanning for Industrial Process Troubleshooting

Marcio Issamu Haraguchi[1], Wilson Aparecido Parejo Calvo[2], Hae Yong Kim[3]

1 - Tricom Tecnologia, Av. Conselheiro Rodrigues Alves, 58, Piquete, Brazil.
2 - Nuclear and Energy Research Institute – IPEN/CNEN-SP, Av. Prof. Lineu Prestes, 2242, São Paulo, SP, Brazil.
3 - Universidade de São Paulo, Escola Politécnica, Av. Prof. Luciano Gualberto, tr. 3, 158, São Paulo, SP, Brazil. Corresponding author.

E-mail: marcio@tricomtecnologia.com.br, waocalvo@ipen.br and hae@lps.usp.br.

Abstract

Gamma scanning is a nuclear inspection technique widely used to troubleshoot industrial equipments in refineries and petrochemicals plants such as distillation columns and reactors. In this technique, a sealed radiation source and detector move along the equipment, and the intensity readouts generate the density profile of the equipment. Although many improvements have been introduced in recent years, the result of gamma scan still consists of a simple 1-D density plot. In this work, we present the tomographic gamma scanning that, using image reconstruction techniques, shows the result as a 2-D image of density distribution. Clearly, an image reveals more features of the equipment than a 1-D graph and many problems that could not be troubleshooted using the conventional technique can now be solved with this imaging technique. We use ART (Algebraic Reconstruction Technique) intercalated with total variation minimization filter. The use of total variation minimization leads to compressive sensing tomography, allowing to obtain good quality reconstruction from few irradiation data. We simulated the reconstruction of different density distributions. We applied the new technique to data obtained by irradiating with gamma rays phantoms that emulate industrial equipments. Finally, we present the result obtained by applying the innovative technique to real operating distillation column. It seems that the new technique has identified a problem in this equipment that is very difficult to detect using conventional gamma scan.

Keywords: gamma scanning, industrial tomography, distillation column, algebraic reconstruction technique, compressive sensing

1 Introduction

In continuous production plants like refineries and petrochemical sites, process equipment performance is analyzed using process model, based on operational variables and quality of product. With increasing complexity and restricted boundaries of design and operation, NDT (Non-Destructive Testing) has been widely used to validate, check and troubleshoot these equipments. Among the available NDTs, nuclear techniques stand out by not disturbing the process under analysis, allowing to carry out tests online. Modern equipments and methods allow nuclear techniques, previously found only in the literature, to be used in industry. Distillation column gamma scanning, neutron backscattering, chemical and radioactive tracers and industrial computerized tomography are powerful techniques that are nowadays commercially available.

Within these technologies, the distillation column profiling or gamma scanning has consolidated as a good option to perform mechanical and operational troubleshooting [1, 2]. In this technique, a radioactive source and detector are positioned in opposite sides of the equipment and move along its length (figure 1). The measured radiation attenuation values result in 1-D longitudinal density profile. Although it relies on simple principles, its practical use is complex due to the required high specific knowledge. This barrier also hinders a wider acceptance by the market, as the final customer must have good experience with the technique. Distillation columns can be found in a wide range of industries such as refineries, fine chemicals, fertilizers and mining plants (figure 2). Inside a distillation column, there are internals parts with tasks such as increasing liquid-vapor contact area, collecting or distributing liquid, heat exchanging, etc.

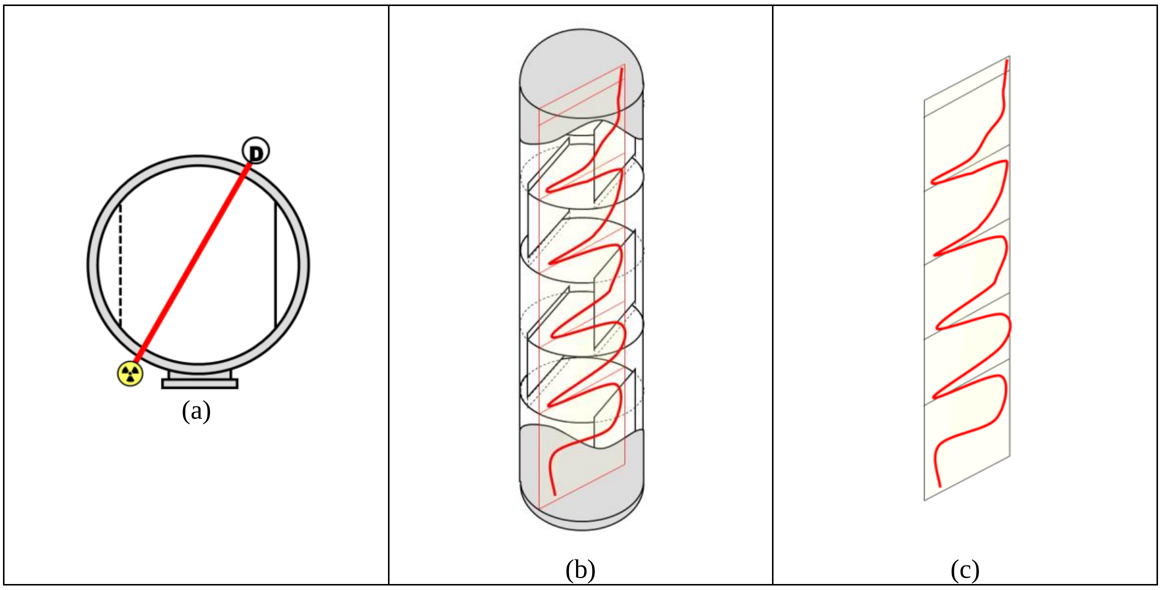

Figure 1. (a) In conventional gamma scanning, the radioactive source and detector are positioned in opposite sides of the equipment. (b) The radiation source/detector move along the column height, obtaining average densities. (c) The results are shown as a 1-D longitudinal density profile.

Figure 2. A typical industrial distillation column.

The inspection industry developed several improvements to gamma scanning to solve technical difficulties and to gain competitive edge, for example: automated scanning, wireless detectors, new data collecting software and improved data presentation. However, none of these techniques yield information of higher quality: the result still consists of a 1-D density profile of the target.

In this paper, we introduce “tomographic gamma scanning”, where the result of gamma scanning is represented as a 2-D image of densities, instead of a 1-D graph. A preliminary version of this work was published as two papers in the Proceedings of 8th World Congress on Industrial Process Tomography [3, 4].

In order to generate 2-D image from gamma ray irradiation data, we use image reconstruction algorithms with specific irradiation geometry (figure 3). This geometry was chosen for practical reasons. The bottom and top regions of industrial equipment may be inaccessible, may have too complex constitution, or may be too far away from the region of interest. In addition, the irradiation cannot be much inclined, because there is always a maximum distance that the rays can cross to yield statistically significant radiation counts. Moreover, the steeper the radiation, the greater the wall thickness the radiation has to cross.

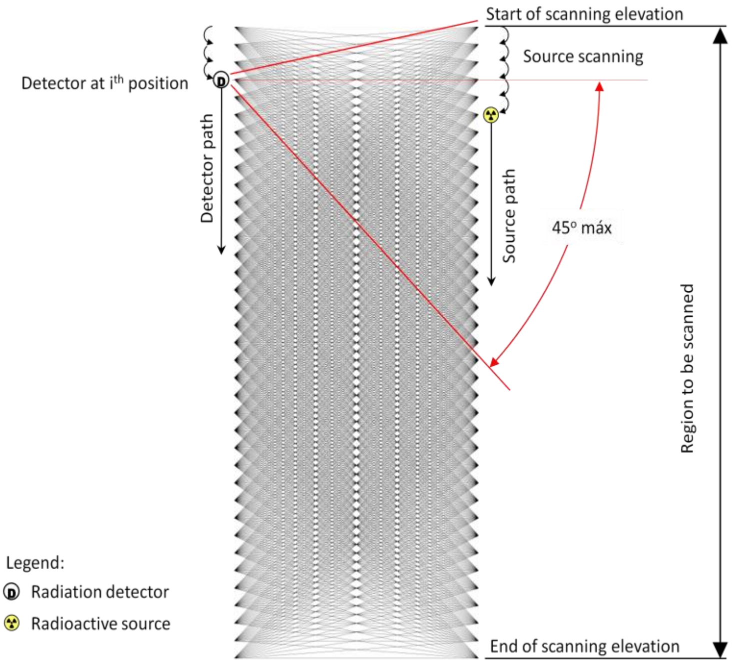

Figure 3. Geometry used in laboratory tomographic scanning, with 5cm spacing and maximum aperture angle of ±45°.

We use ART (Algebraic Reconstruction Technique) [5, 6] intercalated with total variation (TV) minimization filter [7]. The use of this filter allows to obtain good reconstructions even using little irradiation data, and leads to compressive sensing tomography using appropriate parameters [8].

We made reconstructions using simulated data. We applied the new technique to the real data obtained by irradiating gamma rays in phantoms that simulate industrial equipments. Finally, we present the result obtained by applying the new technique to a real industrial installation.

2 Rethinking Gamma Scanning

2.1 Process equipment

The performance of equipments can be analyzed using process models, where input variables are either fixed (equipment size and internal constitution), or can be directly measured (temperature, pressure and flow rate), or calculated (composition of feed, heat consumption and reaction efficiency). The output data are product composition, operational parameters, among others. These models are robust enough to account for the normal measuring errors and parameter variations. However, they cannot account for uncontrolled factors or human errors, such as:

- **Physical:** corrosion, mechanical damage or defective assembly;
- **Process:** contamination, unexpected physical-chemical phenomena, fouling or saturation;
- **Operational:** operational disturbance, instrument reading error or coking;
- **Human:** design problems, badly made repairs or human mistakes.

This is the context where Non-Destructive Testing (NDT) has its main application, allowing to verify the process and troubleshoot the equipment online. Nowadays the use of these techniques has spread beyond the process and operation engineering to other fields of industrial plant engineering:

- **Maintenance:** online evaluation of equipments;
- **Shutdown planning:** opening equipments and supply parts purchasing;
- **Projects and revamps:** critical points verification and performance study;
- **Predictive practices:** critical equipment monitoring.

2.2 Conventional and tomographic gamma scanning

Gamma ray column profiling or gamma scanning is one of the most used NDT techniques [1, 9]. Figure 4 shows an example of a column gamma scan plot.

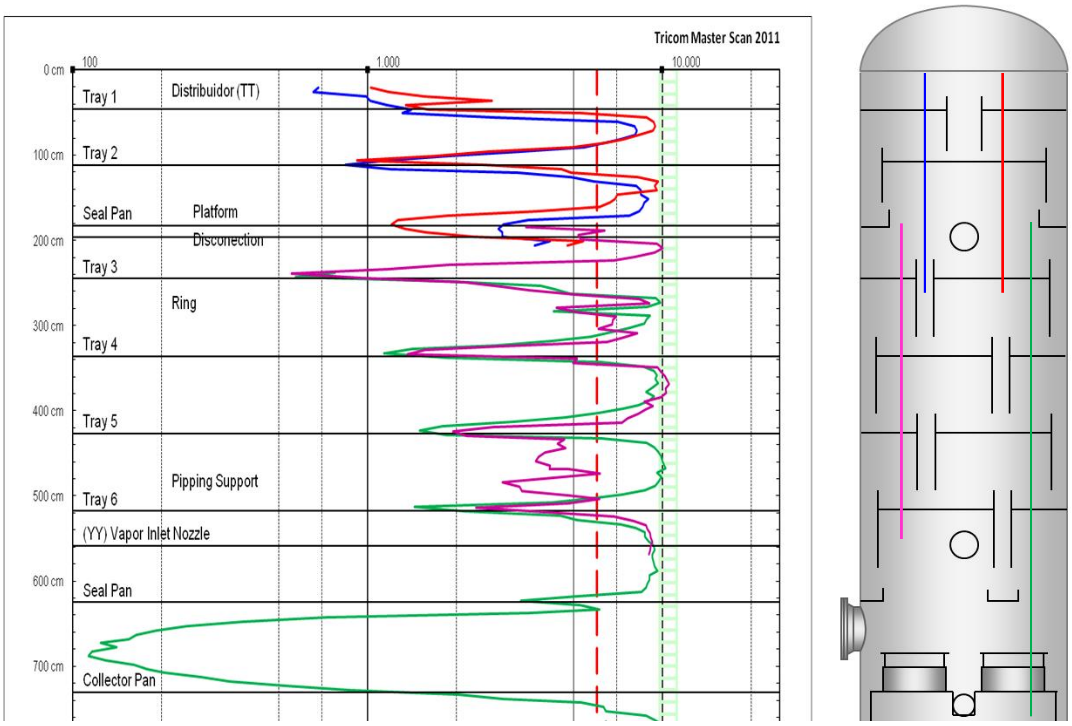

Figure 4. Example of a gamma scan plot. A conventional gamma scan plot represents the density profile of the equipment, with the equipment elevation on the *Y* axis and the relative density values (in counts) on the *X* axis in the log scale. Each color curve represents a density profile measured at the respective color plane shown in the sketch at the right.

Although conceptually simple, gamma scan requires a combination of knowledge, skill and talent of the crew that interfere with the quality of the gathered information and reliability of the conclusions. The required characteristics are so restrict that, historically, the formation of the crew is one of the greatest difficulties faced by the industry.

Column gamma scanning has some technical limitations that may restrict its use, and that cannot be overcome even using the new technique, for example, the radiation count rate. As the time available in field tests is limited, gamma scans are limited to the cases where statistically significant count rates can be obtained. Source activity and energy; detector size and efficiency; equipment size and constitution; and wall thickness must be analyzed to verify the viability of the project. Radiation safety issues are equally relevant [10]. On the other hand, there are many limitations of the conventional gamma scanning that can be overcome using the new technique:

- **Dimensional:** The result of the conventional gamma scan is a 1-D view of the equipment. Multiple scans or grid pattern scans are often used to obtain some spatial notion of the density distribution. Using the tomographic gamma scan, 2-D image of density distribution facilitates the visualization and identification of problem, process and phenomenon of the equipment.
- **Mean density:** Each point of a conventional gamma scan plot represents the mean density along a gamma ray path. In large or tricky equipments, this fact tends to smooth the problem or phenomenon. This limitation can be partially circumvented using baseline scan. Baseline scan can be obtained with the equipment off-line (dry-scan) or online at optimal operational conditions (operational baseline). Using tomographic gamma scan, features hidden in a conventional scan, due to the mean density values, may be revealed. The tomographic gamma scan can also use baseline scanning, because ART image reconstruction algorithms can use the density distribution known a priori.

- **Positioning:** Since the conventional gamma scan is the mean density profile, the interpretation of the obtained data is possible only where the proprieties are held constant during the test along the gamma ray path. This considerably limits the possibilities of positioning gamma ray source and detector. Often, complex equipments are difficult or impossible to be properly scanned. In tomographic gamma scan, the number of profiles can be reduced because a second spatial dimension is added.
- **Interpretation:** Although conventional gamma scan relies on simple principles, the correct interpretation of the result requires high specific knowledge. This barrier also prevents further market acceptance, as the end customer must have good experience with the technique. Images generated by tomographic gamma scan are much easier to understand than the 1-D density plot. This may make easier the acceptance of the inspection by the customer and also facilitate the training of field personal.

3 Gamma Ray Computed Tomography

3.1 Industrial Computed Tomography

Industrial tomography opened new possibilities to troubleshoot industrial equipments [11-14]. Many different physical phenomena can be used to generate tomographic images, for example, electrical capacitance, electrical resistivity, magnetic resonance imaging, x-ray and gamma ray [15]. In particular, gamma ray industrial tomography has been used since at least 1957 [16]. The standard field equipment of industrial gamma ray tomography consists simply of a single radiation source and single or multiple detectors [9, 17-19].

3.2 Tomographic reconstruction problem

Transmission modality is the most common industrial gauge arrangement [9], with a radiation source positioned on one side of an object and a detector on the opposite side. As the gamma ray passes through matter, the beam is attenuated according to Beer-Lambert's exponential decay law:

$$I = I_o e^{-\mu w} \qquad (1)$$

where I is the received radiation intensity, I_o is the emitted radiation intensity, w is the object thickness and μ is the linear attenuation coefficient. The emitted intensity I_o can be determined calibrating the system by measuring intensity I_1 at a distance d_1 and estimating I_0, at the distance d_0, by the law of squares:

$$I_0 = \left[\frac{d_1}{d_0}\right]^2 I_1 \qquad (2)$$

If the attenuation coefficient μ is not constant inside the material, the product μw must be replaced by an integral:

$$\mu w = \int_r \mu(x,y)dr \qquad (3)$$

where $\mu(x, y)$ is the linear attenuation coefficient at point (x,y) measured in cm^{-1} and r is the gamma ray path. Inserting equation (3) and (2) in equation (1):

$$b = -\ln\left(\frac{I}{I_1}\left[\frac{d_0}{d_1}\right]^2\right) = \int_r \mu(x,y)dr \qquad (4)$$

The resulting expression indicates that using the detected radiation intensity I (and knowing the distance d_0, the calibration distance d_1, and the calibration radiation intensity I_1), it is possible to compute the integral of the linear attenuation coefficient along the gamma ray path r. Let us call the term b "measured projection". The tomographic reconstruction problem is to determine the spatial distribution of $\mu(x, y)$ given many measured projections b in many geometrically different ray paths r.

3.3 Tomographic reconstruction algorithms

Many different algorithms can be used to solve tomographic reconstruction problem.

Bartholomew and Casagrande use 4th degree polynomial to represent the distribution of densities, and the polynomial coefficients are obtained by a least-squares algorithm [16]. Obviously, this algorithm can reconstruct only the distribution of densities that can be represented by a 4th degree polynomial and it will not give a "high resolution" image. This algorithm was actually used in industrial tomography [12].

Filtered back projection (FBP) is a popular image reconstruction algorithm and many works use it in industrial gamma ray tomography, for example, Kim et al. [19]. It is also widely used in medical computerized tomographic imaging [20]. It is computationally very efficient. However, a typical FBP implementation requires a large number of radiation measurements to provide a high accuracy in reconstructed images [21]. In our application, the number of measurements is always limited due to the experimental conditions, and so FBP is not adequate.

Iterative reconstruction algorithms are another class of reconstruction algorithm. They are usually more computationally intensive than FBP. However, with appropriate modifications, they can yield good reconstructions even using few irradiation data. In this paper, we use Algebraic Reconstruction Technique (ART) [5, 6]. This algorithm can be considered as iterative solver of a system of linear equations:

$$\boldsymbol{Ax=b} \qquad (5)$$

The values of reconstructed image pixels are the variables of the vector $\boldsymbol{x}$ (the attenuation coefficients $\mu(x, y)$), each row a_i of the matrix $\boldsymbol{A}$ is the path of the i-th gamma ray (the geometry of ray r) and the measured projections form the vector $\boldsymbol{b}$. In simple case, the matrix $\boldsymbol{A}$ consists of only 1's and 0's:

$$a_{ij} = \begin{cases} 1, & \text{if ray } i \text{ passes through pixel } j. \\ 0, & \text{otherwise.} \end{cases} \qquad (6)$$

ART uses the iterative formula below to compute an approximation of the solution of the system of equations:

$$x^{k+1} = x^k + \lambda_k \frac{b_i - \langle a_i, x^k \rangle}{\|a_i\|^2} (a_i)^t \qquad (7)$$

where $i = (k \bmod m) + 1$, λ_k is a relaxation parameter and $\|a_i\|^2$ is the number of pixels that the ray i passes through (number of 1's in a_i).

Replacing $i = (k \bmod m) + 1$ by a randomly chosen index, the randomized ART is obtained. This is the algorithm we actually use in our experiments. Moreover, in our implementation, the relaxation parameter λ_k decreases geometrically as the iteration step k increases.

In industrial tomography and gamma scanning, the expected density distribution of the equipment may be known a priori. This "prior knowledge" can be obtained either by analyzing the drawings of the equipment, its components and understanding the process behavior; or by measuring the baseline density distribution with the equipment off-line or online at optimal operational conditions. ART can easily incorporate this prior knowledge: simply set the initial density distribution x^0 with the expected density distribution. In this case, the problem is to verify whether the obtained data agree (or not) with the prior knowledge. As a practical example, let us say that the walls of the column are dense and thick, and they interfere with the reconstruction, blurring the objects near the walls (as in figure 11a). Using the a priori known wall density (figure 12a), it is possible to obtain a more clear reconstruction (figure 12b), where the dense walls can be seen clearly.

3.4 Compressive sensing computed tomography

Tomographic reconstruction problem in practice does not have a unique solution, because the system of linear equations (5) is usually highly underdetermined, that is, there are much more unknown variables than equations. For example, our real industrial tomographic scanning has 908 data points and 150×360=54000 pixels. Compressive sensing (or compressed sensing) reconstruction tries to minimize the total variation (TV) of the reconstructed image $\mu(x,y)$, that is, the absolute sum (l_1-norm) of the gradient l_2-magnitude of the reconstructed image:

$$\min_{\mu(x,y)} \left\| g_{\mu(x,y)} \right\|_1 \text{ subject to } \boldsymbol{Ax} = \boldsymbol{b} \qquad (9)$$

where $g_{\mu(x,y)}$ is the gradient magnitude of reconstructed image $\mu(x,y)$ in vector form. This minimization will preferably generate piecewise constant reconstructed images.

There are many compressive sensing image reconstruction algorithms [21]. Some of them intercalate a TV minimization filter between the steps of an iterative reconstruction algorithm [8, 21]. We intercalate the TV minimization proposed in [7] between ART iteration steps.

Even before compressive sensing reconstruction algorithms became popular, some authors have proposed to use suitable filters between the steps of iterative reconstruction algorithms. For example, Bustos et al. have proposed to use robust anisotropic diffusion together with MART (Multiplicative ART) [22]. Robust anisotropic diffusion minimizes Tukey's biweight robust error norm [23]. Even simpler filters, such as moving average or median, greatly improves the ART/MART reconstruction quality.

4 Simulation

We implemented ART and the TV minimization filter in C++. We constructed different virtual phantoms to simulate the tomographic gamma scanning. We simulated gamma ray irradiations by computing the Beer-Lambert law attenuation along the ray paths, considering average densities and computing the expected radiation counts in the detector. We can make this simplified simulation, without using sophisticated simulation software such as MCNP (Monte Carlo N-Particle), because we use medium-high energy gamma sources (Cs-137 or Co-60) and NaI(Tl) detectors with energy discrimination settings. Although we made many simulations, in this paper we present only the simulation of a trayed distillation column.

We constructed a virtual phantom of trayed column (figure 5a) and performed a tomographic gamma scan. The external steel walls (in white in figure 5a) were simulated. However, the internal horizontal steel structures (like trays) do not appear in the simulated density distribution. This does not invalidate our simulation, because the source and the detector are not punctual and the system is not collimated. Hence the detector "sees" a radiation beam much larger than the thickness of some horizontal internals. We generated 1179 simulated irradiations, where consecutive positions of radiation source/detector were spaced 5 cm, with maximum aperture angle of ±45° (the maximum angle, in the vertical plane, between source elevation and detector elevation), resulting in 39 fan-shaped projections with 21 to 39 irradiations each (figure 5b). The domain to be reconstructed has dimension 60×190 cm. Phantom materials were air (μ=68×10^{-6} cm^{-1}), water (μ=63×10^{-3} cm^{-1}) and steel (μ=420×10^{-3} cm^{-1}), all linear attenuation values for Co-60. We simulated the radiation counts (I) that would be obtained if a Cobalt 60 source beam, with I_0 intensity, crossed the phantom at every path shown in figure 5b. We scanned the equipment in the direction indicated by blue line in figure 6.

A conventional gamma scan graph was plotted using the tomographic scan data (figure 5c). It indicates dense areas above the trays 2 and 3 and the seal pan (blue dashed circles) that are caused by stacks of liquid in the downcomers. However, it is very difficult to relate them to stacks of liquid, because it is impossible to know the *x*-coordinate of the dense pockets. Thus, in conventional gamma scan, usually the radiation source and detectors are positioned to cross only the active area of the tray (red line in figure 6), since it is very difficult to extract useful information from the downcomers.

We used ART with TV minimization filter to obtain the tomographic reconstruction (figure 5d) that has very good visual quality. It is very easy to see the stacks of liquid in the downcomers in the image. We purposely scanned the equipment in an unusual direction (blue line of figure 6) instead of the usual (red line of figure 6) to demonstrate that the tomographic gamma scan can show features hidden in the conventional scan.

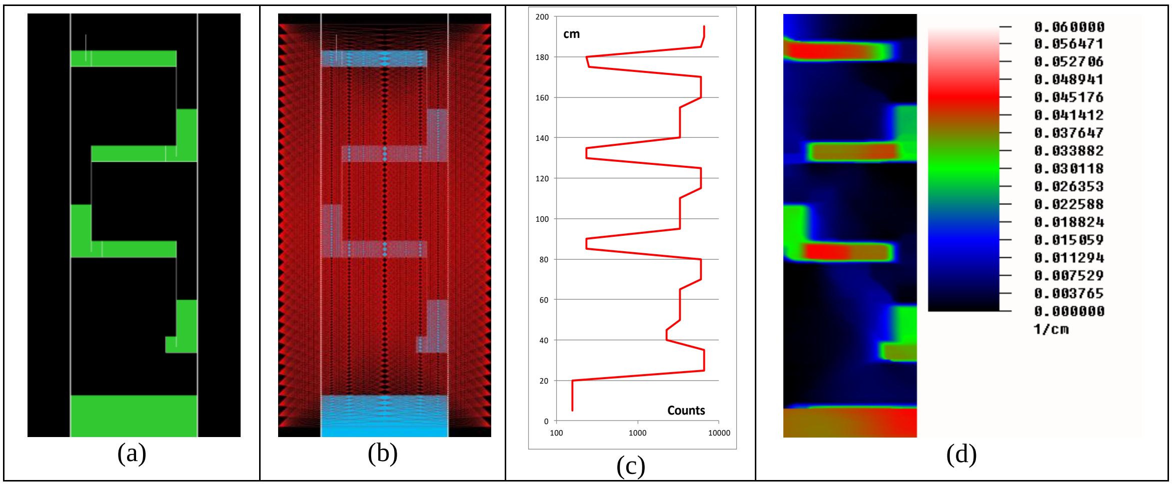

Figure 5. (a) Simulated density distribution of a column, different colors representing different linear attenuation values, black = air (μ=68×10^{-6} cm^{-1}), green = water (μ=63×10^{-3} cm^{-1}) and white = steel (μ=420×10^{-3} cm^{-1}). (b) Simulated tomographic scan geometry. The red lines represent simulated paths of gamma rays. (c) Simulated gamma ray profile. Blue dashed circles are related to the stack of liquid in the downcomers. (d) Simulated tomographic gamma scan. Liquid in the downcomers are easily visible. To facilitate visualization, we use pseudo-colors in the density distribution image.

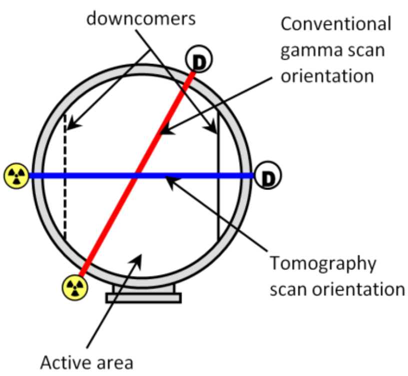

Figure 6. In conventional gamma scan, the radioactive source and detector are usually positioned to cross only the active area of the trays (red line). In tomographic gamma scanning, we positioned the radioactive source and detector to cross the downcomers, in order to demonstrate that the tomographic scan can show features hidden in the conventional scan.

5 Laboratory Experiments

To further test tomographic gamma scanning, we built a mechanical device that automatically collimates the radiation source and detector (figure 7a). This gantry is 2.166 m tall and 1.288 m wide.

We built a physical phantom of trayed column and scanned it perpendicularly to the downcomers (figure 7b). This trayed column has 3 one-pass trays, with 40 cm spacing, 5 cm deep pool (to simulate a 5 cm liquid level), and 5 cm wide downcomer area. The trays were filled with gel balls. The downcomers were also filled with gel balls, up to 20 cm height level.

We also built a physical phantom of random packed column to simulated severe liquid maldistribution with dense and empty regions (figure 7c). The random packed bed was approximately 40 cm high and filled with PVC (polyvinyl chloride) tubes (1 inch in diameter and 2 inches long). It was assembled to simulate typical problems: voids, dense pockets and uneven top.

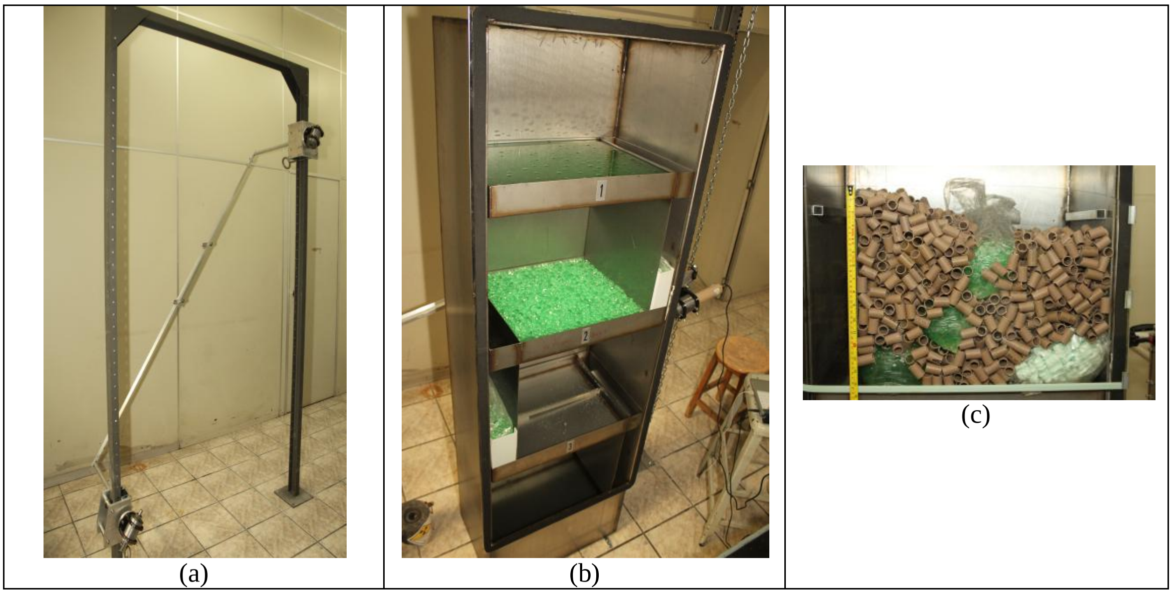

Figure 7. Equipments used in laboratory experiments. (a) The device that automatically aligns the radiation source and detector. (b) A physical phantom that simulates trayed column. (c) A physical phantom that simulates packed column.

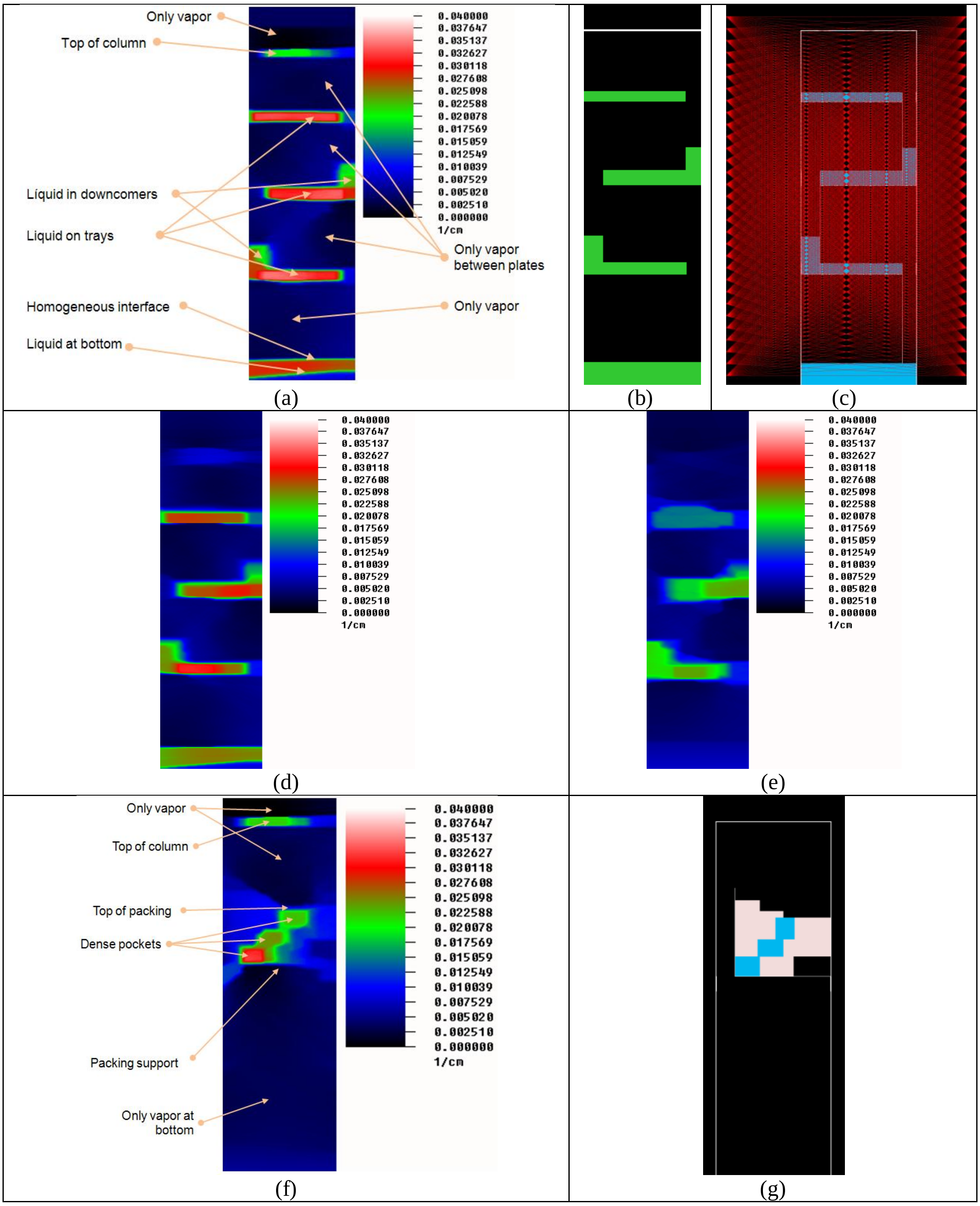

Figure 8. The reconstructions obtained by tomographic gamma scanning, using physical phantoms and real gamma ray irradiations. (a) Reconstruction of trayed column phantom with 5 cm spacing between consecutive positions of radiation source/detector. (b) The expected density distribution of the trayed column (green = water, white = steel, black = air). (c) The irradiation geometry with 5 cm spacing used in tomographic gamma scan - the same geometry was applied to the packed tower. (d) Reconstruction obtained with 10 cm spacing. (e) Reconstruction obtained with 15 cm spacing. (f) Reconstruction of packed column phantom. (g) The expected density distribution of packed column (blue = water, white = steel, black = air, salmon = PVC packing with μ=0.024 cm^{-1}).

Both phantoms are 1.60 m tall and 0.80 m wide, the approximate size of a small industrial distillation column. The phantom walls are made of 3 mm stainless steel plates. We used a Co-60 source with 0.485 mCi activity with 10 mm diameter collimation, and 1 or 2 inch NaI(Tl) detectors with 12.7 mm collimation.

We performed several experiments to check how the recovered image quality changes with the scanning spacing, maximum aperture angle and detector size (1 or 2 inches). Typically, in each experiment, we obtained 1200 irradiation data, each reading took about 3s and the total experiment took about 2 hours, resulting in about 41 fan shaped projections with 24 to 39 irradiations each. Some of the obtained reconstructions are depicted in figure 8.

Some important features, from the point of view of a troubleshooter, can be seen in figure 8a:

- Mechanical integrity of the trays;
- Liquid, vapor and disengagement zone at each tray;
- Presence and height of liquid in the downcomers;
- Presence and shape of liquid level at bottom.

Similarly, the following features, important for a troubleshooter, can be seen in figure 8d:

- Empty regions;
- Dense pockets;
- Unlevered packing.

6 Real Industrial Equipment Tomographic Scanning

The first ever tomographic gamma scanning of real industrial equipment was carried out in a water stripping column located in a petrochemical plant in southern Brazil. The column has 1300 mm internal diameter, walls 9.5 mm thick and is equipped with 10 ripple trays (figure 9). This column has always operated with limitations and was never able to achieve the designed rates and specifications. Several regular gamma scans could not pinpoint any specific problem. Only the top section of the column (containing a 8”-diameter pipe liquid distributor and 6 trays) was scanned using a 6 mCi Co-60 source and a 2×2 inches NaI(Tl) detector, with 10 cm spacing between consecutive positions of radiation source/detector, resulting in 908 data points collected in approximately 2 hours. The total field work was performed in approximately 3 hours, including planning the work, accessing the tower, assembling and disassembling instruments, and data sampling.

As in regular gamma scanning, the results of tomographic scanning can be affected by structures attached to the column, such as rings, nozzles, manways, platforms and supports. The best strategy to avoid such interferences is to choose gamma ray paths away from them. Even if they cannot be avoided, the extra spatial dimension provided by the tomography allows identifying the structure interference in the resulting image. The requirements for accessing the equipment are the same as in regular gamma scanning, so any column that can be scanned by conventional technique can also be analyzed with this technique.

The scans crossed diagonally the liquid distributor at the top (figure 10). A previous conventional gamma scanning of this equipment (figure 11b) was available, and the tomographic scans were performed in the same direction, to allow a direct comparison of the results. In this case, there were no structures attached to the column that could interfere with the results. Mechanical collimation system (similar to the one used in the laboratory) is not practical for field applications due to transportation, assembly and movement difficulties. Thus, we used a non-collimated system with an electronically filtered photopeak energy spectrum, in opposition to the collimated system with wide energy spectrum traditionally employed in gamma scanning industry.

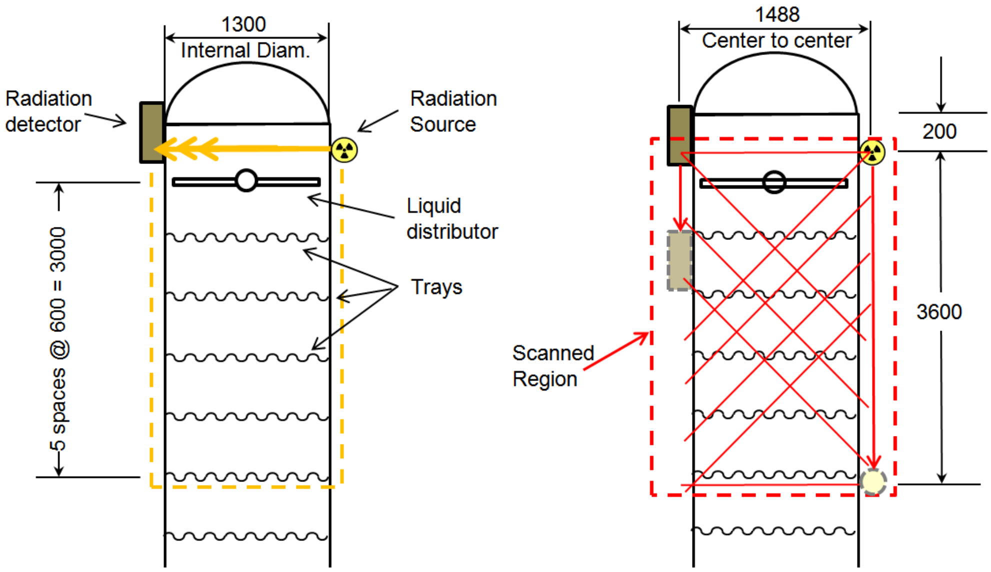

Figure 9. Layout sketch of the scanned water stripping column (dimensions in mm) and tomographic scan geometry.

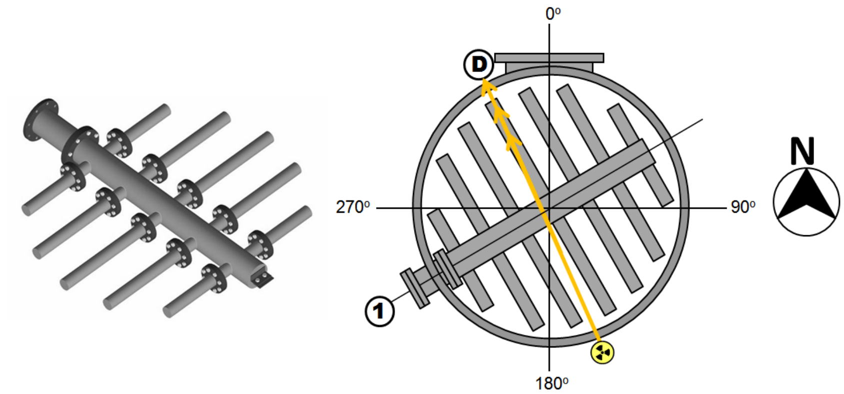

Figure 10. Pipe distributor and scan orientation (source: RASCHIG GmbH. http://www.raschig.de/Pipe-Liquid-Distributor-Type-DP-1).

Figure 11a depicts the result of the tomographic gamma scanning, that is consistent with the conventional scan shown in figure 11b. Image analysis should take into account the ideal operation of each internal part and whether it contains (or not) liquid or aerated liquid. Any deviation from the ideal profile may indicate a mechanical or operational problem. The results of the analysis can be summarized as follows:

- The liquid distributor is in the correct place, with liquid and leveled. The scans crossed it diagonally, so a symmetric shape can be seen at the corresponding elevation, indicating that the central tube and lateral pipes are at their right places.
- An area of low density can be seen above the distributor, indicating that there is no liquid entrainment to the top of the column. Entrainment is a process phenomenon where liquid droplets are carried by vapor flow towards the top of the column. It would be indicated by a higher than normal density in the scan. When properly operating, entrainment should not appear at the top of the column.
- Trays 1 through 5 can be seen at their appropriate elevations. The liquid in the trays seems to be leveled and there are no high densities in the spaces between trays that would indicate entrainment, flooding or other abnormal process phenomena.
- Even numbered ripple trays seem to be denser than odd numbered ones as indicated on both tomographic and conventional gamma scans. Ripple tray assembling explains the difference as even numbered trays are mounted 90 degrees shifted in relation to odd numbered trays. Hence gamma rays cross even ripple trays transversely, hitting the metals of all tray ripples, while they pass almost parallel to the odd tray ripples, hitting mostly aerated liquid.

- The tomographic gamma scan seems to indicate a problem that has never been detected in any previous inspections of this column using conventional gamma scans: trays appear to be less dense at the center. Maldistribution of liquid on the trays may cause this phenomenon, a problem that may occur in ripple trays. Concentric maldistribution of liquid is very difficult to be detected with regular gamma scans. In this case, a regular cross section tomography inspection could confirm (or reject) this hypothesis.

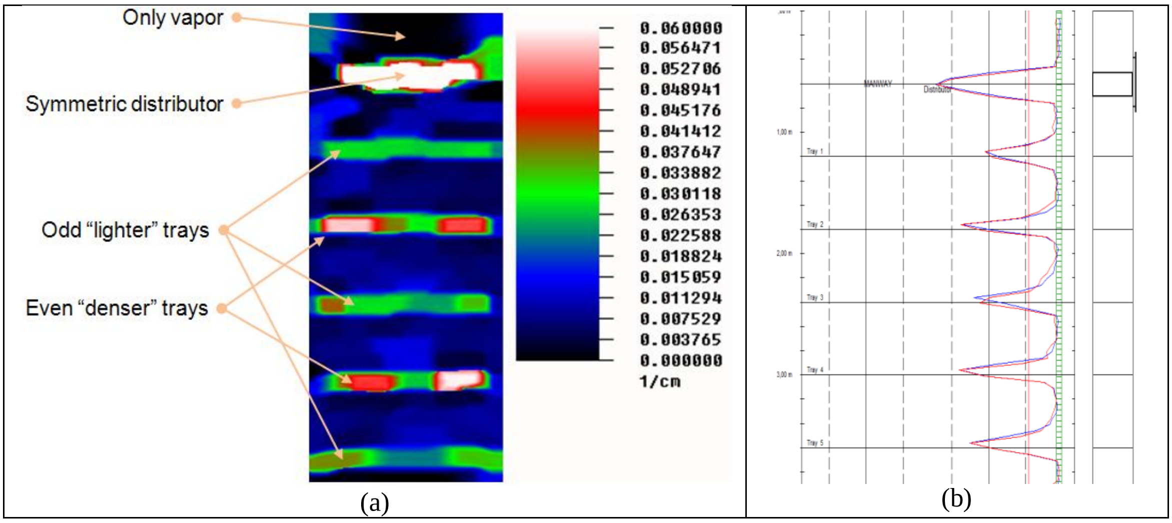

Figure 11. (a) Tomographic gamma scanning of real industrial equipment (without a priori knowledge), performed following the orientation depicted in figure 6. (b) The corresponding conventional gamma scan. Two regular gamma scans, shown as red and blue graphs, were performed at different operational rates following the orientation depicted in figure 6. The vertical red line and the vertical green bar respectively represent the mean densities of liquid and vapor.

Tomographic gamma scan images can be improved using a priori density distribution as the startup point of the reconstruction process. This density distribution can be obtained with the aid of internals details, column operation and process knowledge. Figures 12a and 12b shows respectively the a priori density distribution and the image recovered using this knowledge. The walls of the equipment can be seen perfectly using prior knowledge and the maldistribution of liquid on the trays is even more clearly visible.

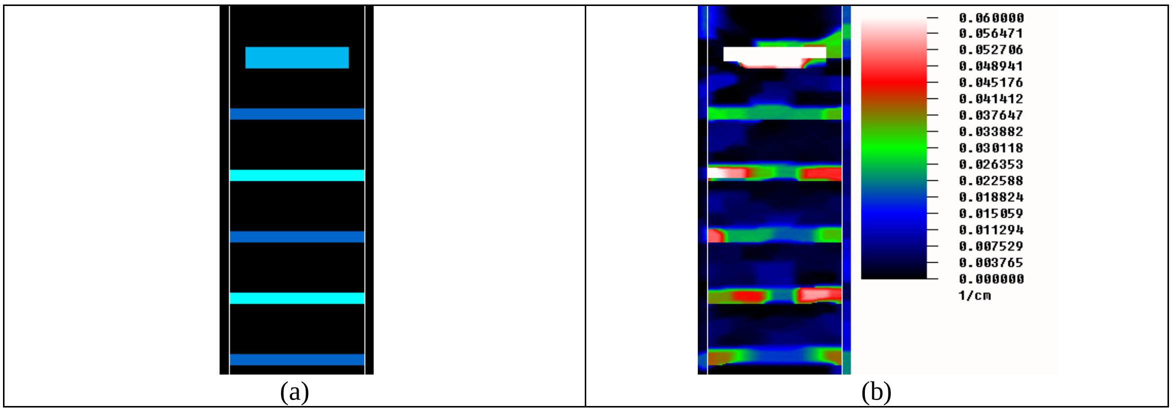

Figure 12. (a) Density distribution known a priori. (b) Reconstruction of the real industrial equipment using a priori knowledge. The walls of the equipment can be seen perfectly and the maldistribution of liquid on the trays is even more clearly visible.

Tomographic gamma scanning can troubleshoot typical abnormalities of the column. We built three column models similar to the real scanned column: with normal trays (figure 13a), with flooded trays (figure 13b) and with damaged trays (figure 13c) and simulated their tomographic scannings. Figure 13 shows the images obtained without prior knowledge. The normal condition image (figure 13a) is similar to the real scanned column and the results indicate that the other two problems would be easily detected with the aid of tomographic images. The simulated reconstruction (figure 13a) do not show any sign of concentric liquid maldistribution.

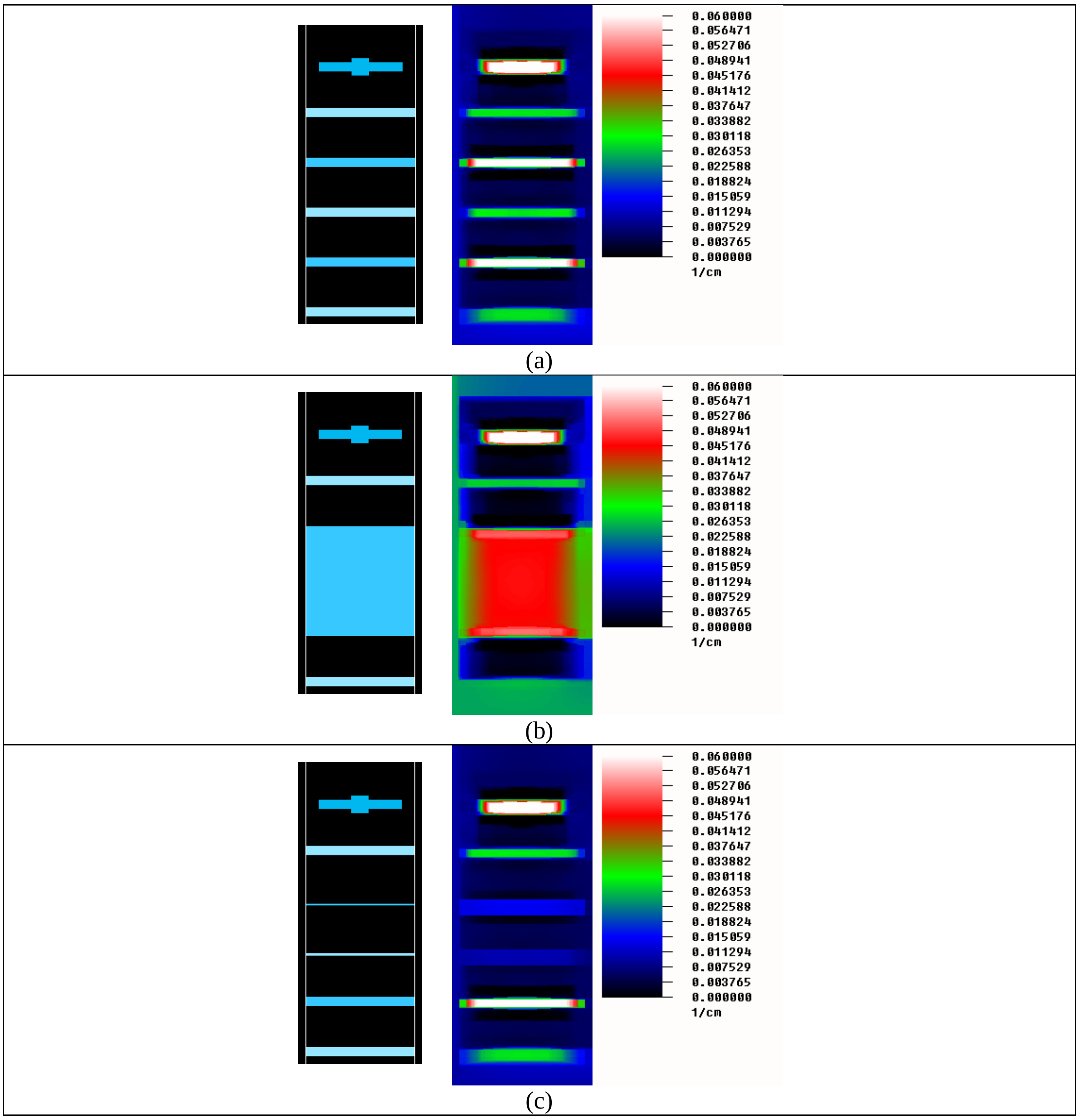

Figure 13. (a) The expected density distribution of the normally operating equipment and the reconstruction. (b) The expected density distribution of the flooded equipment and the reconstruction. (c) The expected density distribution of the damaged equipment and the reconstruction.

7 Acknowledgements

We would like to thank the engineer Francisco Edmundo Sprenger for the design, construction and assembly of the system to align the radiation source and detector. We would like to thank Petrobras and CNPq for the partial financial support of this project through the doctoral scholarship number 163088/2014-4

8 Conclusions

In this paper, we proposed tomographic gamma scanning that uses image reconstruction techniques to generate 2-D image of density distribution of industrial equipments. This technique can detect many features hidden in 1-D density profile generated by a conventional gamma scan, opening new perspectives to solve industrial equipment problems. We used ART (algebraic reconstruction technique) intercalated between the steps of reconstruction algorithms with total variation minimization filter. The use of total variation minimization leads to compressive sensing reconstruction and allows to obtain good reconstructions even using few irradiation data. We simulated the tomographic gamma scanning of a trayed column.

Then, we used the data obtained by irradiating physical phantoms with gamma ray to further test the new technique. Finally, we described the tomographic gamma scanning applied to real operating industrial equipment. In this real test, we could observe signs of possible concentric maldistribution of liquid, which is very difficult to detect using conventional gamma scanning.

References

[1] S.X. Xu, L. Martos, Flooding phenomenon in distillation columns and its diagnosis, part I, trayed columns. *Distillation 2001: Frontiers in a New Millennium, Proc. Topical Conference, AIChE Spring National Meeting*, Houston, TX, 2001.

[2] N.F. Urbanski, M.R. Resetarits, M.S.M. Shakur, Gamma scanning a column containing closely spaced trays. *Annual Meeting AIChE 1999 - Separations Topical Conference*, Dallas, TX, 1999.

[3] M.I. Haraguchi, H.Y. Kim, W.A.P. Calvo, Distillation column troubleshooting with improved gamma scan technique. *8th World Congress on Industrial Process Tomography*, Iguassu Falls, Brazil, 2016.

[4] H.Y. Kim, M.I. Haraguchi, W.A.P. Calvo, Comparison of industrial tomography algorithms for gamma scanning 2-D reconstruction. *8th World Congress on Industrial Process Tomography*, Iguassu Falls, Brazil, 2016.

[5] R. Gordon, R. Bender, G.T. Herman, Algebraic reconstruction techniques (ART) for three-dimensional electron microscopy and x-ray photography. *Journal of Theoretical Biology*, **29(3)** (1970) 471-481.

[6] G.T. Herman, A. Lent, Iterative reconstruction algorithms. *Comput. Biol. Med.*, **6** (1976) 273-294.

[7] A. Chambolle, An algorithm for total variation minimization and applications. *Journal of Mathematical Imaging and Vision*, **20.1-2** (2004) 89-97.

[8] H. Yu and G. Wang, Compressed sensing based interior tomography. *Phys. Med. Biol.*, **54** (2009) 2791-2805.

[9] G.A. Johansen, P. Jackson, *Radioisotope gauges for industrial process measurements*, John Wiley & Sons, 2004.

[10] M.P. Sanches, M.I. Haraguchi, F.S. Beckmann, W.A.P. Calvo, Radiological safety in the gamma scan procedures. *Int. Nuclear Atlantic Conference*, Santos, Brazil, 2007.

[11] A.J. Peyton, M.S. Beck, A.R. Borges, J.E. de Oliveira, G.M. Lyon, Z.Z. Yu, M.W. Brown, J. Ferrerra, Development of electromagnetic tomography (EMT) for industrial applications. Part 1: sensor design and instrumentation. *1st World Congress on Industrial Process Tomography* 306-312, 1999.

[12] S.X. Xu, G. Kennedy, Gamma-ray computer-aided tomography of industrial packed columns. *AIChE Spring National Meeting*, Houston, TX, 1999.

[13] S.X. Xu, Quantitatively measure and assess maldistribution in industrial packed towers. *CE Expo'2000*, Houston, TX, 2000.

[14] T. Wiens, P. Behrens, Turbulent flow sensing using acoustic tomography. *Proc. Innovations in Practical Noise Control*, Ottawa, Canada, 2009.

[15] D.V. Kalaga, A.V. Kulkarni, R. Acharya, U. Kumar, G. Singh, J.B. Joshi, Some industrial applications of gamma-ray tomography. *J. Taiwan Institute of Chemical Engineers*, **40** (2009) 602-612.

[16] R.N. Bartholomew, R.M. Casagrande, Measuring solids concentration in fluidized systems by gamma-ray absorption. *Industrial & Engineering Chemistry*, **49.3** (1957) 428-431.

[17] Technical data on nucleonic gauges, IAEA-TECDOC-1459, July 2005. http://www-pub.iaea.org/MTCD/Publications/PDF/te_1459_web.pdf, accessed on Dec. 2016.

[18] Industrial Process Gamma Tomography, IAEA-TECDOC-1589, May 2008. http://www-pub.iaea.org/MTCD/Publications/PDF/TE_1589_web.pdf, accessed on Dec. 2016.

[19] J. Kim, S. Jung, J. Kim, A study on industrial gamma ray CT with a single source-detector pair. *Nuclear Engineering and Technology*, **38(4)** (2006) 383-390.

[20] X. Pan, E.Y. Sidky, M. Vannier, Why do commercial CT scanners still employ traditional, filtered back-projection for image reconstruction? *Inverse Problems*, **25(12)** (2009) 123009.

[21] A. Biçer, Compressed sensing based computerized tomography imaging, Ph.D. Thesis, Middle East Technical University, 2012.

[22] H.I.A. Bustos, H.Y. Kim, Reconstruction-diffusion: an improved maximum entropy reconstruction algorithm based on the robust anisotropic diffusion. *Brazilian Symp. on Comp. Graph. and Image Processing*, 215-219, 2005.

[23] M.J. Black, G. Sapiro, D.H. Marimont, D. Hegger, Robust anisotropic diffusion. *IEEE Trans. Image Processing*, **7(3)** (1998) 421-432.